



OPEN

Nickel oxide nanoparticles film produced by dead biomass of filamentous fungus

SUBJECT AREAS:

ENVIRONMENTAL
BIOTECHNOLOGY

POLLUTION REMEDIATION

NANOPARTICLES

Marcia Regina Salvadori¹, Cláudio Augusto Oller Nascimento² & Benedito Corrêa¹Received
4 July 2014Accepted
1 September 2014Published
17 September 2014Correspondence and
requests for materials
should be addressed to
M.R.S. (mrsal@usp.br)¹Department of Microbiology, Biomedical Institute II, University of São Paulo, São Paulo, 05508000, Brazil, ²Department of Chemical Engineering, Polytechnic, University of São Paulo, São Paulo, 05508000, Brazil.

The synthesis of nickel oxide nanoparticles in film form using dead biomass of the filamentous fungus *Aspergillus aculeatus* as reducing agent represents an environmentally friendly nanotechnological innovation. The optimal conditions and the capacity of dead biomass to uptake and produce nanoparticles were evaluated by analyzing the biosorption of nickel by the fungus. The structural characteristics of the film-forming nickel oxide nanoparticles were analyzed by scanning electron microscopy (SEM), energy dispersive X-ray spectroscopy (EDS), X-ray photoelectron spectroscopy (XPS), transmission electron microscopy (TEM), and atomic force microscopy (AFM). These techniques showed that the nickel oxide nanoparticles had a size of about 5.89 nm and were involved in a protein matrix which probably permitted their organization in film form. The production and uptake of nickel oxide nanoparticles organized in film form by dead fungal biomass bring us closer to sustainable strategies for the biosynthesis of metal oxide nanoparticles.

Nickel oxide is an important transition metal which has been extensively studied because of its technological applications in magnetic recording media, as a catalyst, and in the medical field. The metal oxide can assume a variety of structural geometries with an electronic structure that can exhibit metallic and semiconductor characteristics, conferring different chemical and physical properties¹.

Nanomaterials have been widely studied over the past decade due their application in different fields such as photoelectric materials, recording media, catalysts, sensors, ceramic materials, and others². In this respect, nickel oxide nanoparticles (NiO NPs) exhibit particular catalytic³ anomalous electronic^{4,5} and magnetic^{6,7} properties. Nanoparticles of NiO with the following shapes have been synthesized: nanotubes, nanobelts, nanorods, hollow spheres, and hexagonal flakes^{8,9}.

Nanotechnology in biology has drawn increasing attention due to its cutting-edge nature and the use of the nanoparticles (NPs) produced in industrial, biomedical and electronic applications such as catalysts¹⁰, in cancer detection¹¹, and as conductors in transistors¹². Biological methods for NPs synthesis can overcome many of the harmful effects of chemical and physical methods, permitting the synthesis of nanomaterials at mild pH, pressure and temperature and at a substantially lower cost.

The fungus-mediated green chemistry approach towards the production of NPs has many advantages, including easy and simple scaling up, economic viability, easy processing and biomass handling, and recovery of large surface areas with optimum growth of mycelia¹³. The live biomass of various fungal genera has been shown to be able to synthesize metal NPs either intracellularly or extracellularly; for example, extracellular NPs production by *Aspergillus fumigatus* (Ag NPs)¹⁴, *Fusarium oxysporum* (Ag NPs)¹⁵, MKY3 (Ag NPs)¹⁶, *Fusarium oxysporum* (Au NPs)¹⁷, *Colletotrichum spp.* (Au NPs)¹⁸, *Verticillium spp.* (magnetite NPs)¹⁹, and *Fusarium oxysporum* (zirconia NPs)²⁰; intracellular NPs production by *Candida glabrata* (CdS NPs)²¹, *Schizosaccharomyces pombe* (CdS NPs)²¹, *Verticillium spp.* (Au NPs)²², *Verticillium spp.* (Ag NPs)²³, *Pichia jadinii* (Au NPs)²⁴, and *Verticillium luteoalbum* (Au NPs)²⁵.

Studies in the literature have reported the use of dead fungal biomass for the synthesis of transition metal NPs, such as the extracellular synthesis of copper NPs by *Hypocrea lixii*²⁶ and the intracellular synthesis of copper NPs by the yeast *Rhodotorula mucilaginosa*²⁷. This study reports for the first time the synthesis and uptake of NiO NPs organized in film form by dead biomass of the filamentous fungus *Aspergillus aculeatus* (*A. aculeatus*). This natural production of NPs is a unique environmentally friendly process.



Results

The filamentous fungus *A. aculeatus* was isolated from the area of a copper mine in the Amazon region. Analysis of minimum inhibitory concentrations revealed that the fungus exhibited a high tolerance to nickel (up to 1473 mg/L). Dead, dried and live biomass of *A. aculeatus* was able to produce NiO NPs from Ni (II) in aqueous solution, with a maximum uptake capacity of the metal of 19.6 mg/g, 6.2 mg/g and 5.2 mg/g, respectively. The best physicochemical conditions of nickel sorption for the three types of biomass were a contact time of 90 min, initial pH 4.0, temperature of 30°C, agitation speed of 150 rpm, initial Ni (II) concentration of 100 mg/L, and biosorbent dose of 1.0 g. The efficiency of nickel uptake was 89.02%, 53.25% and 48.26% for dead, dried and live biomass, respectively. The Langmuir model was used to describe the nickel (II) biosorption isotherm for the three types of biomass. The isotherm constants, maximum loading capacity estimated by the Langmuir model, and regression coefficients are shown in Table 1.

The NiO NPs (produced extracellularly by the dead fungal biomass) were characterized by morphological and structural analysis. The Figs. 1a and 1b shows the SEM photomicrographs before and after the synthesis of NiO NPs by dead fungal biomass, respectively. Modification of the fungal surface occurred as a result of the formation of a film coating the surface of the fungal biomass after binding to the NiO NPs (Fig. 1b). The EDS spectra in Figs. 1c and 1d show the region of the mycelium before and after nickel exposure, respectively. Fig. 1d shows the signals of nickel in the fungus. Signals of C, N and O were also observed, indicating the possible presence of proteins as a capping material on the surface of the NPs. This protein matrix may be responsible for the stabilization (capping material) and organization of the NPs in the form of a film on the biomass surface. Figs. 1e and 1f shows the images of the live fungal biomass before and after synthesis of NiO NPs, respectively. The Figs. 2a and 2b shows the two-dimensional (2D) images of dead *A. aculeatus* biomass in the absence and presence of NPs, respectively. Three-dimensional (3D) images of dead biomass impregnated or not with NPs are shown in Figs. 2c and 2d, respectively. The formation of a smooth film of NiO NPs coating the surface of dead fungal biomass can be seen in both AFM images (2D and 3D) in which the biomass was impregnated with NPs. The Figs. 2e and 2f shows the AFM images (2D) of the live biomass without and with presence of the NPs, respectively and 3D Figs. 2g and 2h of the live biomass without and impregnated with NPs, respectively.

The Fig. 3 shows the XPS spectrum of the Ni ($2p_{3/2}$) core level of the NiO NPs forming a film on the surface of *A. aculeatus*. The peak at 854.1 eV corresponds to the Ni $2p_{3/2}$ level and is characteristic of NiO^{28,29}. There was no peak at 852.2 eV, which would be characteristic of the Ni $2p_{3/2}$ level of Ni (0)³⁰. In the core level O 1 s and N 1 s the major binding energies at 532.6 eV and 400 eV (data not shown) respectively were observed confirming the presence of proteins involving NiO NPs. This results corroborated with the observed in EDS spectra, which suggests the possibility of these agents acting as capping agents³¹ that would be associated with the organization of the NiO NPs in the film form. The Fig. 4 shows the TEM image of the NiO NPs synthesized extracellularly by the dead biomass of *A. aculeatus* in the cell wall surface showing an average diameter of 5.89 nm and NPs predominantly spherical.

Discussion

The fungi has the capacity to survive metals toxicity by means of mechanisms produced in direct response to metal species concerned. The *A. aculeatus* presented a tolerance to the nickel metal transition (up to 1473 mg/L) due to the mechanism biosorption through fungal cell wall. The fungal biomass walls are formed of chitin, chitosan, glucan, lipid, phospholipids, which contain carboxyl groups, amino groups phosphates, lipids, melanin, sulphates and hydroxides^{32,33}, these functional groups are the sites sorption of the metals^{34–37}. Dead biomass exhibited the highest capacity to produce NiO NPs from Ni (II) through biosorption. The present results showed that dead *A. aculeatus* biomass had a higher adsorption capacity (19.6 mg/g) than those described for other known biosorbents, such as *Trichoderma harzianum* (11.77 mg/g), *Rhizopus arrhizus* (9.28 mg/g), *Aspergillus terreus* (7.86 mg/g), *Aspergillus niger* (7.69 mg/g), *Aspergillus flavus* (7.5 mg/g), *Alternaria alternata* (7.37 mg/g), *Cunninghamella echinulata* (4.69 mg/g)³⁸, and macro fungi *Lactarius salmonicolor* (14.90 mg/g)³⁹. Studies suggest that, at higher concentrations, Ni ions interact with cellular components such as organic acids⁴⁰, nucleotides⁴¹, amino acids⁴², phospholipids⁴³, etc resulting in the disturbance of physiological and biochemical processes. There are few studies reporting^{26,27} the use of dead fungal biomass to produce metal NPs. However, dead biomass has advantages such as its limited toxicity, the possibility of storage for a prolonged period of time, and the fact that it does not require growth media and nutrients for its maintenance. Morphological analysis of the NiO film formed by NiO NPs on the fungal surface by SEM and AFM provided cross-sectional images of the sample (2D SEM image in Fig. 1b and 2D and 3D AFM images in Figs. 2b and 2d). Both techniques revealed the smooth characteristic of the film of NiO NPs. There are no reports in the literature on NiO NPs produced by dead fungal biomass forming this film structure. EDS analysis showed elements that may be derived from biomolecules, such as proteins, provided by the fungal biomass surrounding the NiO NPs. This analysis was confirmed by the XPS results. Fungal cell proteins were possibly released during the autoclaving process and bound on the cell surface²⁶. Proteins probably act as a capping agent in the formation of NiO NPs³¹, constituting a protein matrix around the NiO NPs that possibly confers their arrangement in film form. However, the type and mechanism of action of the proteins involved in these processes remain to be studied.

The electron micrograph reveals a NiO NPs profile produced by a green process using dead fungal biomass with average diameter of 5.89 nm. Similar results have been reported in previous studies^{44,45} producing Ag and others NPs, but using live fungal biomass. In summary, the present study explored for the first time the production and uptake of NiO NPs produced by dead biomass of *A. aculeatus*. These NPs formed a film on the biomass surface. This natural method provides low-cost, rapid and economically friendly process for the formation and uptake of NiO NPs. In a next step, we intend to characterize the biomolecules that are involved in the production of NiO NPs and the arrangement of these NPs in the formation of the film.

Methods

Growth and maintenance of the organism. *A. aculeatus* was isolated from the water collected in a copper wastewater pond at the Sossego mine, located in Canãa dos Carajás, Pará, Brazilian Amazonia region (06° 26' S latitude and 50° 4' W longitude). The fungus was maintained and activated on Sabouraud Dextrose Agar (SDA) (Oxoid, England)⁴⁶.

Analysis of nickel (II) tolerance. The tolerance of the isolated fungus to nickel was determined as the minimum inhibitory concentration (MIC) by the spot plate method⁴⁷. SDA plates containing different nickel concentrations (50 to 2000 mg/L) were prepared and inocula of the fungus were spotted onto the metal and control

Table 1 | Adsorption constants from simulation with Langmuir model

Type of biomass	Langmuir model		
	q_m (mg/g)	b (L/mg)	R^2
Live	5.2	0.013	0.987
Dried	6.2	0.017	0.989
Dead	19.6	0.024	0.996

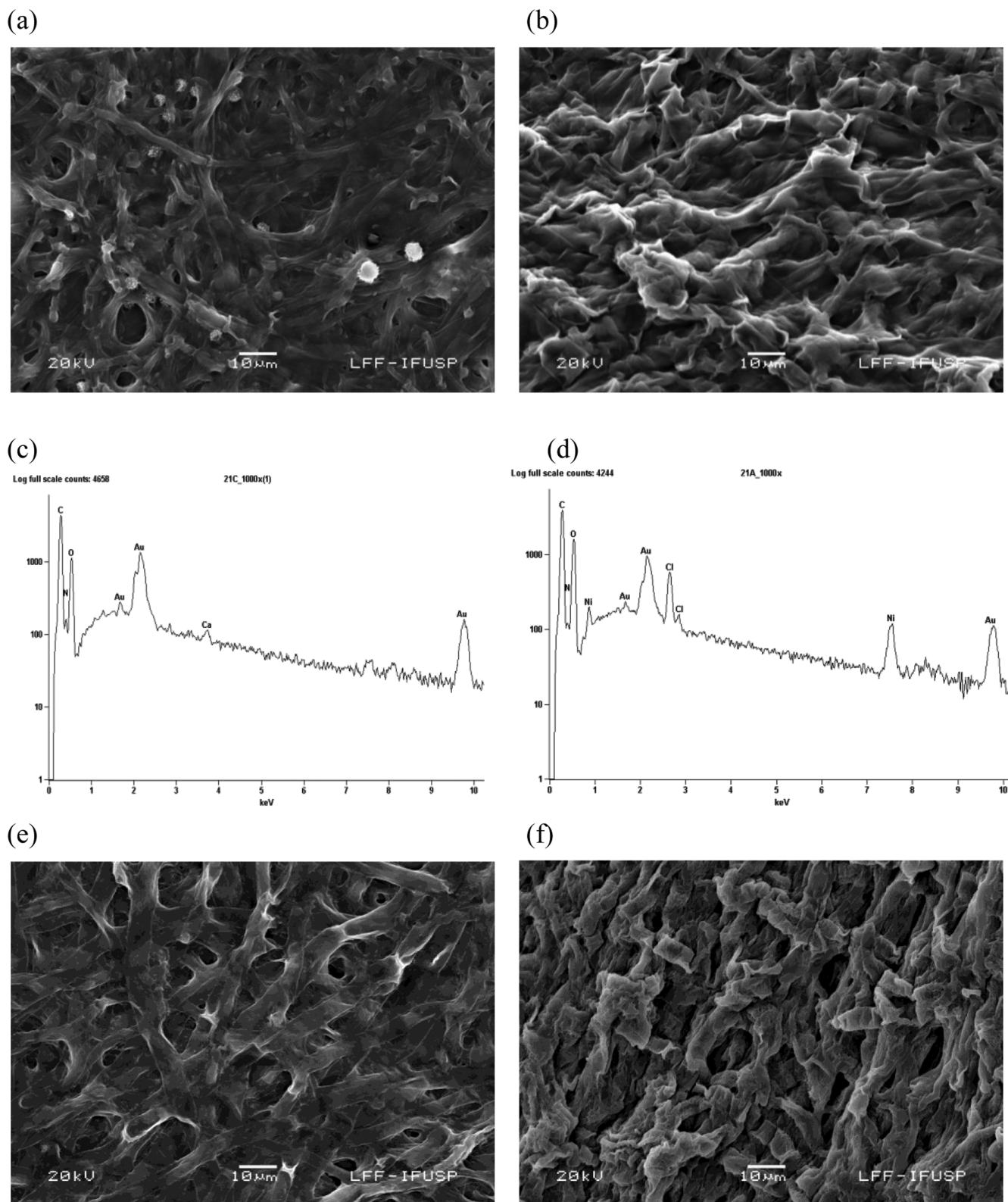


Figure 1 | SEM images of the surface of dead and live *A. aculeatus* biomass, and EDS spectra of the dead biomass. (a) SEM micrograph before the adsorption of nickel by dead biomass, (b) SEM micrograph showing the formation of a film coating the surface of the dead fungal biomass after binding to the NiO NPs. (c) EDS spectrum before exposure of dead biomass to the nickel solution, (d) EDS spectrum after exposure of the dead biomass to the metal, confirming the presence of nickel, (e) SEM micrograph before adsorption of nickel by live biomass and (f) SEM micrograph showing the live fungal biomass, after binding to the NiO NPs.

plates (plate without metal). The plates were incubated at 25°C for 5 days. The MIC is defined as the lowest concentration of metal that inhibits visible growth of the isolate.

Preparation of the adsorbate solutions. All chemicals used in the present study were of analytical grade and were used without further purification. All dilutions were prepared in double-deionized water (Milli-Q Millipore 18.2 MΩcm⁻¹ resistivity).

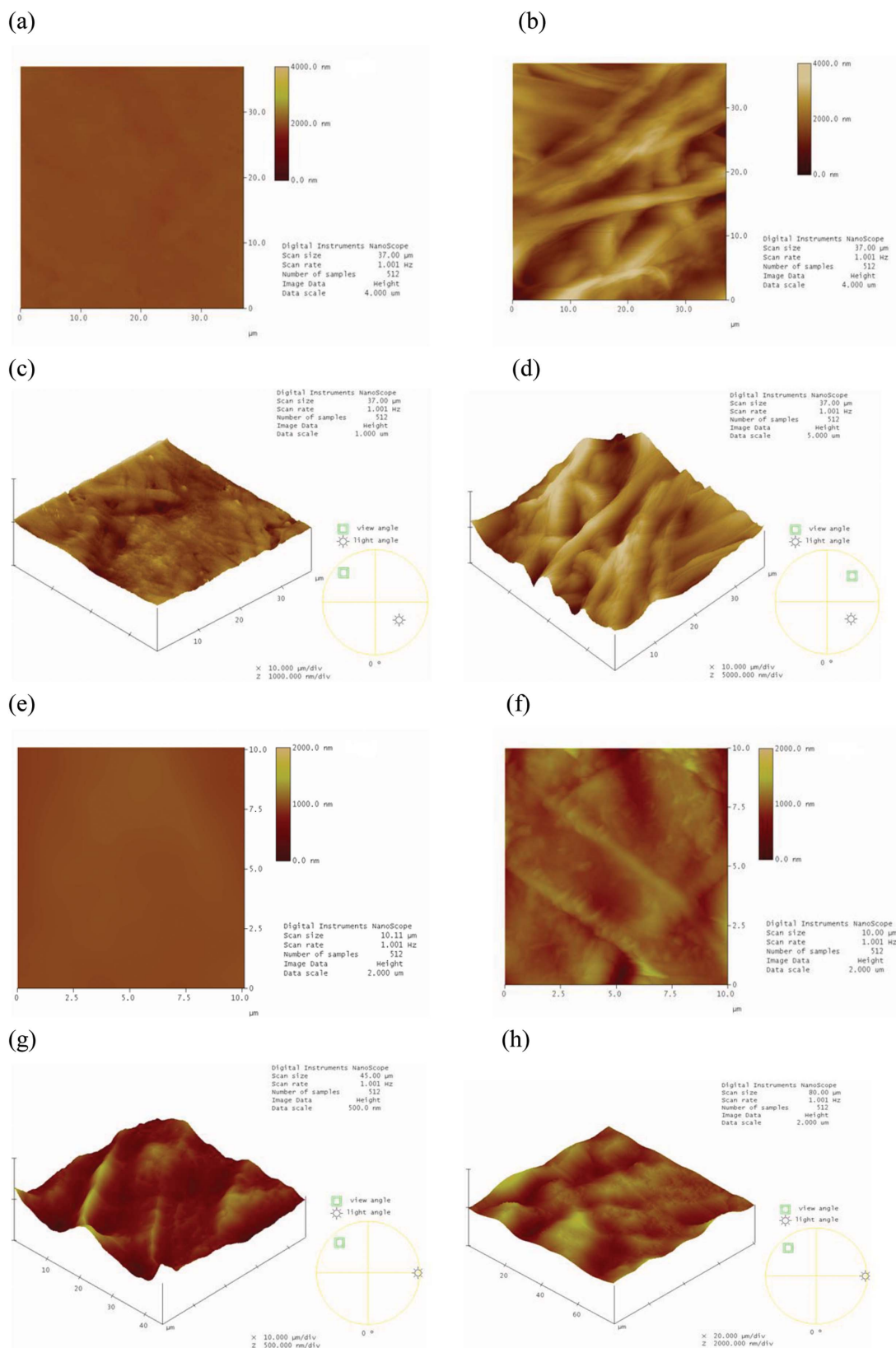


Figure 2 | AFM images of the surface of dead and live *A. aculeatus* biomass. (a) AFM image (2D) of the dead fungal biomass without NiO NPs, (b) AFM image (2D) of the dead fungal biomass impregnated with NiO NPs, showing the formation of a film coating the surface of the dead fungal biomass, (c) AFM image (3D) showing the dead fungal biomass without NiO NPs, (d) AFM image (3D) showing the dead fungal biomass after impregnation with NiO NPs which form a film on the surface of the dead biomass, (e) AFM image (2D) showing the live fungal biomass without NiO NPs, (f) AFM image (2D) showing the live fungal biomass impregnated with NiO NPs, (g) AFM image (3D) showing the live fungal biomass without NiO NPs and (h) AFM image (3D) showing the live fungal biomass after impregnation with NiO NPs.

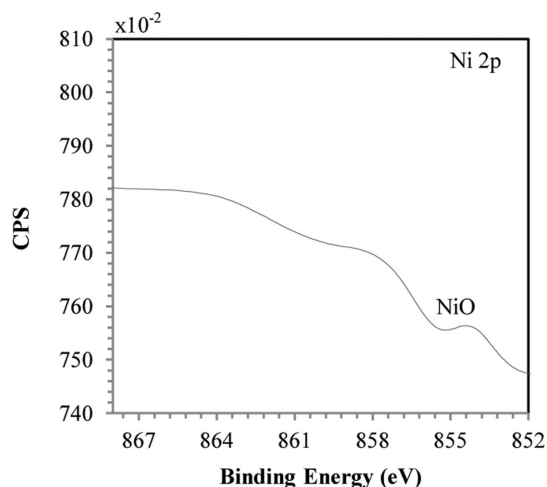


Figure 3 | XPS spectrum of the NiO NPs that compose the film.

The nickel stock solution was prepared by dissolving $\text{NiCl}_2 \cdot 6\text{H}_2\text{O}$ (Carlo Erba, Italy) in double-deionized water. The working solutions were prepared by diluting this stock solution.

Biomass preparation. The fungal biomass was prepared in Sabouraud broth (Sb) (Oxoid, England) and incubated at 25°C for 5 days, at 150 rpm. After incubation, the pellets were harvested and washed with double-deionized water. This preparation is referred to as live biomass. For the preparation of dead biomass, an appropriate amount of live biomass was autoclaved. The dried biomass was obtained by drying the fungal mat at 50°C until it became crispy. The dried mat was ground to obtain uniform sized particles²⁶.

Analysis of the effects of physicochemical parameters on the adsorption efficiency of NiO NPs onto the biosorbent. The effect of pH (2–6), temperature (20 – 60°C), contact time (5–300 min), initial nickel concentration (50–500 mg/L), agitation rate (50–250 rpm), and biosorbent dose (0.15–1.25 g) on the removal of nickel was analyzed. These experiments were optimized using 45 mL of a Ni (II) test solution (100 mg/L) in plastic flask. Different nickel (II) concentrations were prepared by appropriate dilution of the nickel (II) stock solution. The pH of the solution was adjusted using HCl or NaOH. The desired biomass dose was then added and the content of the flask was shaken. After shaking, the Ni (II) solution was separated from the biomass by vacuum filtration through a Millipore membrane. The metal concentration in the filtrate was determined by inductively coupled plasma-optical emission spectrometry. The efficiency (R) of metal removal was calculated using the following equation (1):

$$R = (C_i - C_e) / C_i \cdot 100 \quad (1)$$

where C_i and C_e are initial and equilibrium metal concentrations, respectively. The metal uptake capacity, q_e , was calculated using the following equation (2):

$$q_e = V(C_i - C_e) / M \quad (2)$$

where q_e (mg/g) is the biosorption capacity of the biosorbent at any time, M (g) is the biomass dose, and V (L) is the volume of the solution.

Sorption isotherm. The Langmuir equilibrium model⁴⁸ was used to fit Ni (II) biosorption isotherm experimental data, as follows:

The linearized Langmuir isotherm model according to equation (3):

$$C_e / q_e = 1 / (q_m \cdot b) + C_e / q_m \quad (3)$$

where q_m is the monolayer sorption capacity of the sorbent (mg/g), and b is the Langmuir sorption constant (L/mg).

Characterization of the NiO NPs. In this study, dead biomass of *A. aculeatus* was used which showed a high adsorption capacity of nickel compared to live and dried biomass. The NiO NPs were synthesized by dead *A. aculeatus* biomass using the following conditions: contact time of 90 min, initial pH 4.0, temperature of 30°C , agitation speed of 150 rpm, biosorbent dose of 1.0 g, and a solution containing 100 mg/L Ni (II). The surface morphology of the NiO film formed by NiO NPs produced by the dead and live biomass was examined by SEM (JEOL 6460 LV). The dead biomass was examined by energy dispersive spectrometer (EDS) to identify the composition of elements of the sample and the dead and live biomass by AFM Icon Nanoscope V (Bruker). Transmission electron microscopy (TEM) (JEOL-1010) was used to observe the microstructure of the NiO NPs forming the film, such as size and shape. The chemical state of nickel in the film was analyzed by XPS. The XPS analysis was carried out at a pressure of less than 10^{-7} Pa using a commercial spectrometer

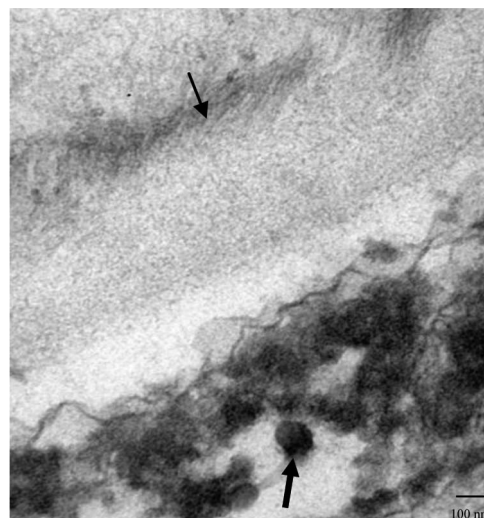


Figure 4 | TEM micrograph of dead *A. aculeatus* biomass. Section of the fungus showing extracellular localization of the NiO NPs (darkest arrow) in the cell wall (lighter arrow).

(UNI-SPECS UHV System). The Mg $K\alpha$ line was used ($h\nu = 1253.6$ eV) and the analyzer pass energy was set to 10 eV. The inelastic background of the electron core-level spectra was subtracted using Shirley's method. The composition (at.%) of the near surface region was determined with an accuracy of $\pm 10\%$ from the ratio of the relative peak areas corrected by Scofield's sensitivity factors of the corresponding elements. The spectra was fitted without placing constraints using multiple Voigt profiles.

- Patil, V. *et al.* Effect of annealing on structural, morphological, electrical and optical studies of nickel oxide thin films. *JSEMAT*. **1**, 35–41 (2011).
- Conte, M., Prossini, P. P. & Passerini, S. Overview of energy/hydrogen storage: state-of-the-art of the technologies and prospects for nanomaterials. *Mater. Sci. Eng. B*. **108**, 2–8 (2004).
- Dooley, K. M., Chen, S. Y. & Hoss, J. R. H. Stable Nickel-Containing Catalysts for the Oxidative Coupling of Methane. *J. Catal.* **145**, 402–408 (1994).
- Biju, V. & Khadar, M. A. Analysis of AC electrical properties of nanocrystalline nickel oxide. *Mater. Sci. Eng. A*. **304**, 814–817 (2001).
- Soriano, L., Abbate, M., Vogel, J. & Fuggle, J. C. The electronic structure of mesoscopic NiO particles. *Chem. Phys. Lett.* **208**, 460–464 (1993).
- Kodama, R. H., Makhlof, S. A. & Berkowitz, A. Finite Size Effects in Antiferromagnetic NiO Nanoparticles. *Phys. Rev. Lett.* **79**, 1393–1396 (1997).
- Kodama, R. H. Magnetic nanoparticles. *J. Magn. Magn. Mater.* **200**, 359–372 (1999).
- Puntes, V. F., Krishnan, K. M. & Alivisatos, A. P. Colloidal nanocrystal shape and size control: The case of cobalt. *Science* **291**, 2115–2117 (2001).
- Liu, Z. *et al.* Complex-Surfactant-Assisted Hydrothermal Route to Ferromagnetic Nickel Nanobelts. *Adv. Mater.* **22**, 1946–1948 (2003).
- Hashmi, A. S. K. & Hutchings, G. J. Gold Catalysis. *Angew. Chem. Int. Ed.* **45**, 7896–7936 (2006).
- Huang, X. H., Jain, P. K., El-Sayed, I. H. & El-Sayed, M. A. Gold nanoparticles: interesting optical properties and recent applications in cancer diagnostic and therapy. *Nanomedicine*. **2**, 681–693 (2007).
- Wu, Y. L., Li, Y. N., Liu, P., Gardner, S. & Ong, B. S. Studies of gold nanoparticles as precursors to printed conductive features for thin-film transistors. *Chem. Mater.* **18**, 4627–4632 (2006).
- Varshney, R., Bhadauria, S. & Gaur, M. S. A review: Biological synthesis of silver and copper nanoparticles. *Nano Biomed. Eng.* **4**, 99–106 (2012).
- Bhainsa, K. C. & D' Souza, S. F. Extracellular biosynthesis of silver nanoparticles using the fungus *Aspergillus fumigatus*. *Colloids Surf. B: Biointerf.* **47**, 160–164 (2006).
- Ahmad, A. *et al.* Extracellular biosynthesis of silver nanoparticles using the fungus *Fusarium oxysporum*. *Colloids Surf. B: Biointerf.* **28**, 313–318 (2003).
- Kowshik, M. *et al.* Extracellular synthesis of silver nanoparticles by a silver-tolerant yeast strain MKY3. *Nanotechnology*. **14**, 95–100 (2003).
- Mukherjee, P. *et al.* Extracellular synthesis of gold nanoparticles by the fungus *Fusarium oxysporum*. *Chem. Biochem.* **3**, 461–463 (2002).
- Shankar, S. S., Ahmada, A., Pasrichaa, R. & Sastry, M. Bioreduction of chloroaurate ions by geranium leaves and its endophytic fungus yields gold nanoparticles of different shapes. *J. Mater. Chem.* **13**, 1822–1826 (2003).
- Bharde, A. *et al.* Extracellular biosynthesis of magnetite using fungi. *Small* **2**, 135–141 (2006).



20. Bansal, V., Rautaray, D., Ahmad, A. & Sastry, M. Biosynthesis of zircônia nanoparticles using the fungus *Fusarium oxysporum*. *J. Materials Chem.* **14**, 3303–3305 (2004).
21. Dameron, C. T. *et al.* Biosynthesis of cadmium sulphide quantum semiconductor crystallites. *Nature* **338**, 596–597 (1989).
22. Mukherjee, P. *et al.* Bioreduction of AuCl₄ ions by the fungus, *Verticillium sp.* and surface trapping of the gold nanoparticles formed. *Angew Chem. Int.* **40**, 3585–3588 (2001).
23. Senapati, S. *et al.* Fungus mediated synthesis of silver nanoparticles: A novel biological approach. *Indian J. Phys.* **78A**, 101–105 (2004).
24. Gericke, M. & Pinches, A. Microbial production of gold nanoparticles. *Gold Bull.* **39**, 22–28 (2006a).
25. Gericke, M. & Pinches, A. Biological synthesis of metal nanoparticles. *Hydrometallurgy*. **83**, 132–140 (2006b).
26. Salvadori, M. R., Lepre, L. F., Ando, R. A., do Nascimento, C. A. O. & Corrêa, B. Biosynthesis and uptake of copper nanoparticles by dead biomass of *Hypocrea lixii* isolated from the metal mine in the Brazilian Amazon region. *Plos One* **8**, 1–8 (2013).
27. Salvadori, M. R., Ando, R. A., do Nascimento, C. A. O. & Corrêa, B. Intracellular biosynthesis and removal of copper nanoparticles by dead biomass of yeast isolated from the wastewater of a mine in the Brazilian Amazonia. *Plos One* **9**, 1–8 (2014).
28. Song, P., Wen, D., Guo, Z. X. & Korakianitis, T. Oxidation investigation of nickel nanoparticles. *Phys. Chem. Chem. Phys.* **10**, 5057–5065 (2008).
29. Lee, S. *et al.* Ni/NiO core/shell nanoparticles for selective binding and magnetic separation of histidine-tagged proteins. *J. Am. Chem. Soc.* **128**, 10658–10659 (2006).
30. Furstenau, R. P., McDougall, G. & Langell, M. A. Initial stages of hydrogen reduction of NiO(100). *Surf. Sci.* **150**, 55–79 (1985).
31. Bansal, V., Ahamad, A. & Sastry, M. Fungus-mediated biotransformation of amorphous silica in rice husk to nanocrystalline silica. *J. Am. Chem. Soc.* **128**, 14059–14066 (2006).
32. Caesartonthat, T. C., Kloke, F. V., Geesey, G. G. & Henson, J. M. Melanin production by filamentous soil fungus in response to copper and localization of copper sulfide by sulfide-silver staining. *Appl. Environ. Microbiol.* **61**, 1968–1975 (1995).
33. Kapoor, A., Viraraghavan, T. & Cullimore, D. R. Removal of heavy metals using the fungus *Aspergillus niger*. *Bioresour. Technol.* **70**, 95–104 (1999).
34. Mullen, M. D., Wolf, D. C., Beveridge, T. J. & Bailey, G. W. Sorption of heavy metals by soil fungi *Aspergillus niger* and *Mucor rouxii*. *Soil Biol. Biochem.* **24**, 129–135 (1992).
35. Kapoor, A. & Viraraghavan, T. Heavy metals biosorption site in *Aspergillus niger*. *Bioresour. Technol.* **61**, 221–227 (1997).
36. Sarret, G. *et al.* Structural determination of Pb binding sites in *Penicillium chrysogenum* cell wall by EXAFS spectroscopy and solution chemistry. *J. Synchrotron Radiat.* **6**, 414–416 (1999).
37. Zhou, J. L. Zn biosorption by *Rhizopus arrhizus* and other fungi. *Appl. Microbiol. Biotechnol.* **51**, 686–693 (1999).
38. Shoaib, A., Naureen, A., Tanveer, F. & Aslam, N. I. Removal of Ni(II) Ions from Substrate using Filamentous Fungi. *Inter. J. Agr. & Bot.* **14**, 831–833 (2012).
39. Akar, T., Celik, S., Ari, A. G. & Akar, S. T. Nickel removal characteristics of an immobilized macro fungus: equilibrium, kinetic and mechanism analysis of the biosorption. *J. Chem. Technol. Biotechnol.* **1**, 1–10 (2012).
40. Cataldo, D. A., McFadden, K. M., Garland, T. R. & Wildung, R. E. Organic constituents and complexation of nickel (II), iron (III), cadmium (II) and plutonium (IV) in soybean xylem exudates. *Plant Physiol.* **86**, 734–739 (1988).
41. Brintzinger, H. The structures of adenosine triphosphate metal ion complexes in aqueous solution. *Biochem. Biophys. Acta.* **77**, 343–345 (1963).
42. Leberman, R. & Robin, B. R. Metal complexes of histidine. *Trans. Faraday Soc.* **55**, 1660–1670 (1957).
43. Hendrickson, H. S. & Fullington, J. G. Stabilities of metal complexes of phospholipides: Ca (II), Mg (II) and Ni (II) complexes of phosphatidylserine and triphosphoinositide. *Biochemistry* **4**, 1599–1605 (1965).
44. Vigneshwaran, N. *et al.* Biological synthesis of silver nanoparticles using the fungus *Aspergillus flavus*. *Mater. Lett.* **61**, 1413–1418 (2007).
45. Basavaraja, S. S., Balaji, S. D., Lagashetty, A. K., Rajasab, A. H. & Venkataraman, A. Extracellular biosynthesis of silver nanoparticles using the fungus *Fusarium semitectum*. *Mater. Res. Bull.* **43**, 1164–1170 (2008).
46. Kumar, B. N., Seshadri, N., Ramana, D. K. V., Seshiah, K. & Reddy, A. V. R. Equilibrium, Thermodynamic and Kinetic studies on *Trichoderma viride* biomass as biosorbent for the removal of Cu (II) from water. *Separ. Sci. Technol.* **46**, 997–1004 (2011).
47. Ahmad, I., Ansari, M. I. & Aqil, F. Biosorption of Ni, Cr and Cd by metal tolerant *Aspergillus niger* and *Penicillium sp* using single and multi-metal solution. *Indian J. Exp. Biol.* **44**, 73–76 (2006).
48. Volesky, B. Biosorption process simulation tools. *Hydrometallurgy*. **71**, 179–190 (2003).

Acknowledgments

This work was supported by the Fundação de Amparo à Pesquisa do Estado de São Paulo (FAPESP). The authors are very much thankful to the Laboratory of Photoelectron Spectroscopy (LEFE), Universidade Estadual Paulista “Júlio de Mesquita Filho” (UNESP), Araraquara, São Paulo, Brazil, by the performing the XPS analysis in this research work.

Author contributions

M.R.S. conceived the experiments. M.R.S. designed and performed the experiments, and analysed the data. M.R.S., C.A.O.N. and B.C. discussed the data and wrote the paper.

Additional information

Competing financial interests: The authors declare no competing financial interests.

How to cite this article: Salvadori, M.R., Nascimento, C.A.O. & Corrêa, B. Nickel oxide nanoparticles film produced by dead biomass of filamentous fungus. *Sci. Rep.* **4**, 6404; DOI:10.1038/srep06404 (2014).



This work is licensed under a Creative Commons Attribution-NonCommercial-NoDerivs 4.0 International License. The images or other third party material in this article are included in the article's Creative Commons license, unless indicated otherwise in the credit line; if the material is not included under the Creative Commons license, users will need to obtain permission from the license holder in order to reproduce the material. To view a copy of this license, visit <http://creativecommons.org/licenses/by-nc-nd/4.0/>